REPORT DOCUMENTATION PAGE

Form Approved
OMB NO. 0704-0188

1. AGENCY USE ONLY (Leave Blank)	2. REPORT DATE 17 July 2000	3. REPORT TYPE AND DATES COVERED 15 April 1998-14 April 1999

4. TITLE AND SUBTITLE
Frictional Characteristics of Cracks and Failure of Brittle Materials Under Dynamic Compression

5. FUNDING NUMBERS
DAAG55-98-1-0229

6. AUTHOR(S)
Guruswami Ravichandran

7. PERFORMING ORGANIZATION NAME(S) AND ADDRESS(ES)
California Institute of Technology
Graduate Aeronautical Laboratories
Pasadena, CA 91125

8. PERFORMING ORGANIZATION REPORT NUMBER GR-ARO-98-44

9. SPONSORING / MONITORING AGENCY NAME(S) AND ADDRESS(ES)
U. S. Army Research Office
P.O. Box 12211
Research Triangle Park, NC 27709-2211

10. SPONSORING / MONITORING AGENCY REPORT NUMBER
ARO 38833.1-EG

11. SUPPLEMENTARY NOTES
The views, opinions and/or findings contained in this report are those of the author(s) and should not be construed as an official Department of the Army position, policy or decision, unless so designated by other documentation.

12 a. DISTRIBUTION / AVAILABILITY STATEMENT
Approved for public release; distribution unlimited.

12 b. DISTRIBUTION CODE

13. ABSTRACT (Maximum 200 words)

A newly developed specimen has been used to investigate the compressive failure due to the presence of flaws in brittle materials. Experiments were conducted under both static and dynamic loading conditions to delineate the role of friction on sliding induced crack initiation. Specimens with different coefficients of friction and crack inclination were prepared and a systematic understanding of crack initiation under compressive loading has emerged. The onset of crack growth is dynamic even under quasi-static loading conditions and the crack initiation is suppressed by presence even small amounts of lateral confinement.

14. SUBJECT TERMS
Solid Mechanics; compressive failure; friction; dynamic loading; fracture; numerical simulations

15. NUMBER OF PAGES
9

16. PRICE CODE

17. SECURITY CLASSIFICATION OR REPORT	18. SECURITY CLASSIFICATION ON THIS PAGE	19. SECURITY CLASSIFICATION OF ABSTRACT	20. LIMITATION OF ABSTRACT
UNCLASSIFIED	UNCLASSIFIED	UNCLASSIFIED	UL

Frictional Characteristics of Cracks and Failure of Brittle Materials Under Dynamic Compression

ARO Grant # DAAG55-98-1-0229
15 April 1998-14 April 1999
G. Ravichandran (PI)
California Institute of Technology

Scientific Personnel
G. Ravichandran (PI)
S. Lee (Postdoctoral Scholar)

Final Report

Abstract
Crack initiation in brittle materials under biaxial compression was studied experimentally under both quasi-static and dynamic conditions with particular attention to the frictional characteristics of the microcracks. Two pieces of Homalite-100 (a brittle polymer) were bonded except for a central region that served as a central crack. The crack surface roughness and hence the friction coefficient μ was varied by polishing and sandblasting. *In situ* photoelastic fringes were obtained and compared with numerical results. Numerical model that accounted for frictional interaction between crack surfaces showed that the shear traction at failure initiation was uniform along most (90%) of the crack surfaces and there was no relative (sliding) displacement near crack tips.

Introduction

Dynamic crack initiation and growth in brittle materials under *tension* has been investigated extensively both analytically and experimentally. However, relatively little is known regarding dynamic cracking phenomena under compression in brittle materials such as ceramics. Also, in numerous applications such as lightweight armor, failure occurs through cracking under multiaxial compression. Hence, there is a need to understand the response of cracks subjected to compression especially their resistance to sliding under transient loading conditions.

Brittle materials such as ceramics and rocks can fail catastropically under compressive loading through the initiation, propagation and coalescence of microcracks [1,2]. An important parameter governing the compressive failure of brittle materials is the frictional resistance of the microcracks to sliding. Such sliding results in developing local tensile stresses at the tips of a microcrack leading to tension cracks at the microcrack tip [1].

However there is very few experimental results concerning the frictional resistance to sliding in such materials. Only a few experiments have been performed under quasi-static conditions for studying crack initiation in brittle materials under far-field compression [1,3]. Due to the qualitative nature of these experiments they do not provide validity of the existing models [1,2, 4] for initiation and propagation of cracks under compression. Currently, only analytical models exist concerning crack initiation under dynamic loading conditions [e.g., 5, 6]. The predictions for compressive strength of the material for realistic values of the parameters in the existing models usually over-predict the compressive strength by a significant factor. One of the reasons for this could be attributed to the assumption of uniform shear stress along the crack surfaces.

Recently, efforts have been made to relax these restrictive assumptions in studying failure of solids under far-field compression [7, 8]. A recent investigation [7] suggests that the discrepancies may be due to the assumptions concerning the frictional resistance of cracks under compression. To the best of authors' knowledge, no experimental results are available for crack initiation and propagation under compressive loading.

In this paper crack initiation in brittle materials under biaxial compression was studied experimentally under both quasi-static and dynamic loading conditions with particular attention to the frictional characteristics of the microcracks as well as the parameters governing crack initiation and propagation.

Quasi-static loading

Specimens In order to study the frictional characteristics of microcracks two pieces of Homalite-100 (a brittle polymer) were bonded except for a central region that served as a central crack. However, since the adhesive is of finite thickness, crack surfaces can not be in contact before loading if the surfaces are flat. Thus bonding portion of the surface was machined to be slightly deeper by 0.1 mm than unbonded portion as shown in Figure 1, thus ensuring that the crack surfaces were in contact prior to loading. The surface roughness of the central region was varied by polishing and sandblasting. The friction coefficient, μ, of polished and sandblasted surface was measured to be 0.38 and 0.7, respectively. It was also varied to create a non-uniform surface roughness with the central 60% of the crack being rough and the rest of the crack close to the tips to be smooth.

The plates were 5 mm thick, 89 mm high and 38 mm wide with a crack length of 11 mm. Specimens were prepared with the bonded interface at angles, ϕ, of 30, 45, 60, and 75° to the major compression loading axis.

Experimental results Both uniaxial and biaxial compression experiments were conducted. The plates were loaded in axial compression with edge-guides to prevent buckling. Quasi-static uniaxial compression experiments showed that the crack initiation load was higher for higher friction coefficient for a given orientation (ϕ) of the crack as shown in Figure 2. The compressive failure stress σ_f is normalized by $K_{Ic}/\sqrt{\pi c}$ where K_{Ic} is the fracture toughness of Homalite. The failure stress for μ=0.38 closely matches the results presented by Ashby and Hallam [9]. Following initiation, cracks began to grow in an unstable (dynamic) manner in the direction of compression until the length of wing crack was about 3 times the initial crack length. The initial direction of the wing crack was between 70 and 80° from the direction of initial crack.

Biaxial compression tests were performed by applying a constant lateral compression before applying an axial compressive load. The failure stresses under biaxial loading conditions are listed in Table 1. The results in Table 1 are slightly different from the failure stress under uniaxial compression. The normalized failure stress $\sigma_f \sqrt{\pi c} / K_{Ic}$ for non-uniform surface roughness has average value 12.2. Though 60 percent of crack surface is rough, the failure stress is close to that of uniformly smooth surface.

In situ photoelastic fringes (isochromatics) were obtained from the tests in order to determine the profile of shear traction on the crack surfaces. Isochromatic fringes under the same compressive load are shown in Figure 3 for different friction coefficients. Comparison of fringes shows that the stress intensity factor is higher for smaller friction coefficient, μ=0.38 under the same compressive load. For smaller μ, the sliding resistance is lower as can be seen from Figure

2 and the stress intensity is induced at the crack tip is higher leading to lower crack initiation load.

μ	σ_2 [MPa]	$\sigma_f\sqrt{\pi c}$ / K_{Ic}
0.38	0.0	9.0
	0.9	10.0
	1.5	10.3
0.70	0.0	14.0
	0.9	15.2
	1.5	16.2

Table 1. Failure stress under biaxial compression

Numerical analysis The lower half of the pictures in Figure 3 is the result of nonlinear finite element analysis with a commercial program ABAQUS. Fringes from numerical results match very well with those from experiments. Plates under compression were modeled as shown in Figure 4. The CPS8 element used is an eight-node plane stress element. Frictional interaction between crack surfaces was accounted for during the analysis. The friction model in ABAQUS allows the introduction of a shear stress limit, which is the maximum value of shear stress that can be carried by the interface before the surfaces begin to slide [10]. The output includes contact pressure, frictional shear stress and contact status. The contact status may be open, closed and sticking tangentially, or closed and sliding tangentially.

Traction on crack surface Contact pressure and shear stress distributions are shown in Figure 5. Under small compression most of crack surface is closed and sticking tangentially so that shear stress is below the critical shear stress μp, where p is the value of contact pressure. As compression increases crack surfaces start to slide from central region so that shear traction reaches the critical value. In Figure 6 the normal and shear traction profiles at crack initiation are shown. The shear traction was uniform along the most (90%) of the crack surface. However, the shear traction becomes smaller approaching the crack tip because surfaces near crack tip are sticking. When the plate is confined laterally (σ_2 = 1.3Mpa), sliding of crack surfaces is restricted as shown in Figure 7(a). Traction on the surface with non-uniform friction coefficient is shown in Figure 7(b). The central region (60% of crack) is rough (μ=0.70) and the rest of the crack surface is smooth (μ=0.38). It is shown that slippage occurs first at weaker section (smooth region).

Dynamic loading

Both uniaxial and biaxial compression experiments were conducted under dynamic (impact) loading. Specimens with a pre-crack are impacted using a drop-weight tower or an air gun, depending on proper impact velocity of projectile. If impact velocity is too low or high, crack does not initiate or specimens are shattered from impact side of the specimen. Air gun was used for laterally confined specimens. The experimental setup for dynamic (impact) experiments is shown in Figure 8. Specimens have width 63.5 mm and height 89 mm with 11 mm-long center crack that is oriented at 45° angle (ϕ) to the major compression axis. A tapered piece of steel

was attached to the impact end of the specimen with a thin layer of vacuum grease. It was confirmed from photoelastic fringes that stress wave was uniformly distributed over the specimen cross-section as shown in Figure 9.

In uniaxial compression tests drop-weight tower was used to impact specimens. Impact velocity was 4.8m/s. Tension-induced wing cracks also appeared under impact loading. Photoelastic fringes around dynamically growing cracks are recorded using a high-speed camera with framing rates of up to 2 million frames/s. Isochromatic fringes at crack initiation for different crack surface roughness are shown in Figure 9 and 10. Fringe patterns are very similar to those from quasi-static tests.

Summary

A newly developed specimen has been used to investigate the compressive failure due to the presence of flaws in brittle materials. Experiments were conducted under both static and dynamic loading conditions to delineate the role of friction on sliding induced crack initiation. Specimens with different coefficients of friction and crack inclination were prepared and a systematic understanding of crack initiation under compressive loading has emerged. The onset of crack growth is dynamic even under quasi-static loading conditions and the crack initiation is suppressed by presence even small amounts of lateral confinement.

Bibliography

1. Horii, H. and Nemat-Nasser, S. (1986) "Brittle failure in compression: splitting, faulting and ductile-brittle transition," *Philosophical Transactions of the Royal Society, London,* 319, 337-374.
2. Ashby, M. F. and Sammis, C. G. (1990) "The damage mechanics of brittle solids in compression," *Pure and Applied Geophysics,* 133, 489-521.
3. Venkinis, G., Ashby, M. F. and Beaumont, P. W. R. (1991) "Compressive failure of alumina containing controlled distribution of flaws," *Acta Metallurgica et Materialia,* 39, 2583-2588.
4.Lehner, F. and Kachanov, M. (1996) "On modeling of wing cracks under compression," *International Journal of Fracture,* 77, R69-R75.
5. Ravichandran, G. and Subhash, G. (1995) "A micromechanical model for high strain-rate behavior of ceramics," *International Journal of Solids and Structures,* 32, 2627-2646.
6. Wright, T. W. and Ravichandran, G, (1996) "On shock induced damage in ceramics," *Contemporary Research in the Mechanics and Mathematics of Materials,* eds: R. C. Batra and M. F. Beatty, CIMNE, Barcelona, Spain, 480-488
7. Wright, T. W. (1997) Private communication
8. Bhattacharya, K., Ortiz, M. and Ravichandran, G. (1998) "Energy-based model of compressive splitting in heterogeneous brittle solids," *Journal of the Mechanics and Physics of Solids,* 46, 2171-2181.
9. Ashby, M. F. and Hallam, S. D. (1986) "The failure of brittle solids containing small cracks under compressive stress states," *Acta metall,* 34, 497-510.
10. Hibbitt, Karlsson and Sorensen, Inc. (1996) *ABAQUS Theory Manual, Version 5.6.*

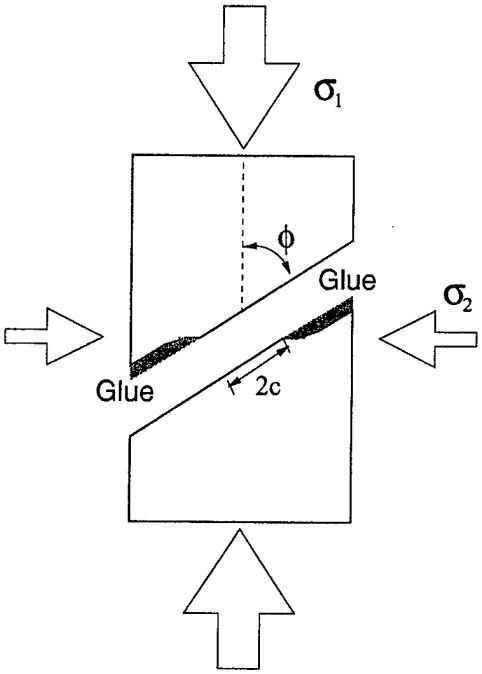

Figure 1 Specimen

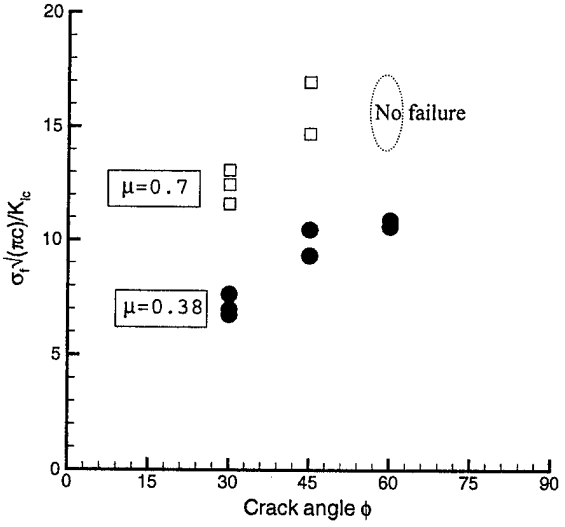

Figure 2. Failure stress under uniaxial compression

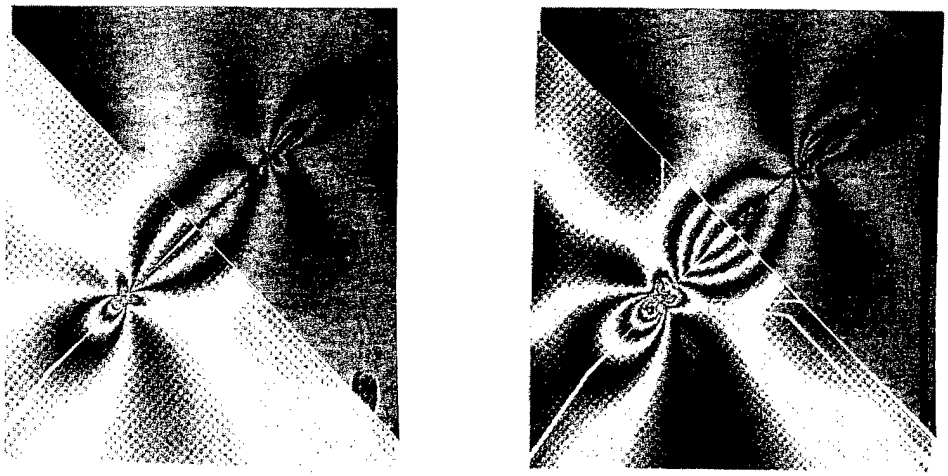

$\mu = 0.7$ $\mu = 0.38$

Figure 3. Comparison of isochromatic fringes from experiment and computation under uniaxial compression $\sigma_1 = 22.9$ MPa

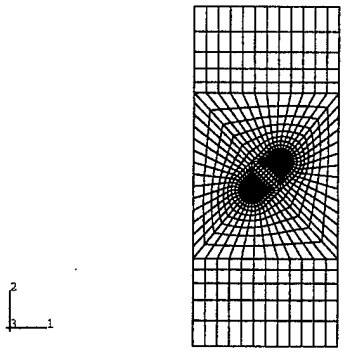

Figure 4. Finite element mesh for plates ϕ=45°

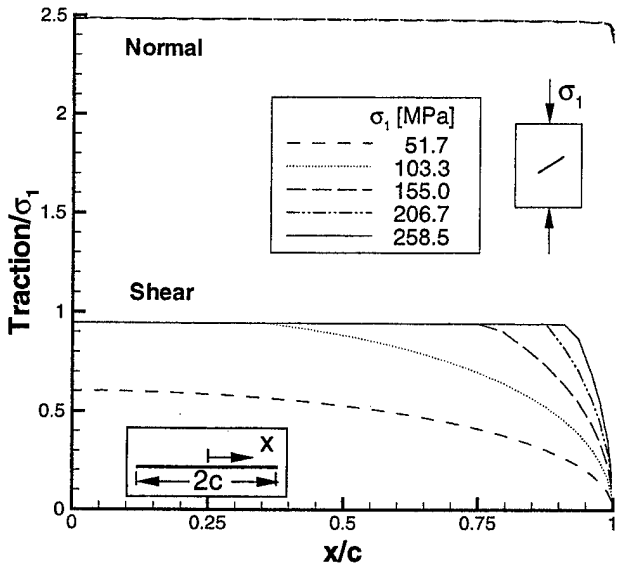

Figure 5. Normal and frictional shear stresses along crack surfaces under unaxial compression (crack angle $\phi = 45^{\circ}$, $\mu = 0.38$)

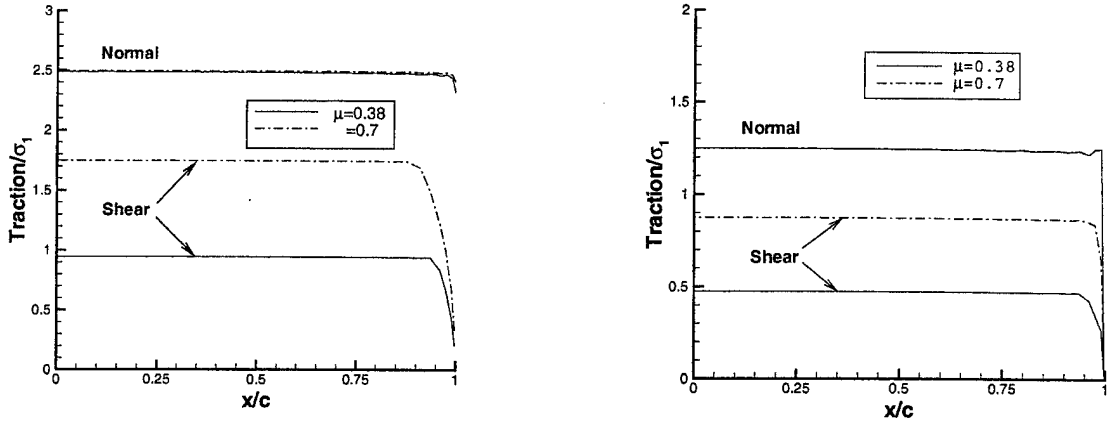

(a) $\phi = 45^{\circ}$ (b) $\phi = 60^{\circ}$

Figure 6. Normal and frictional shear stresses along crack surfaces at failure initiation

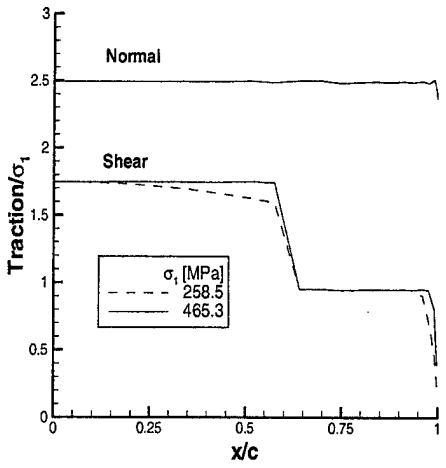

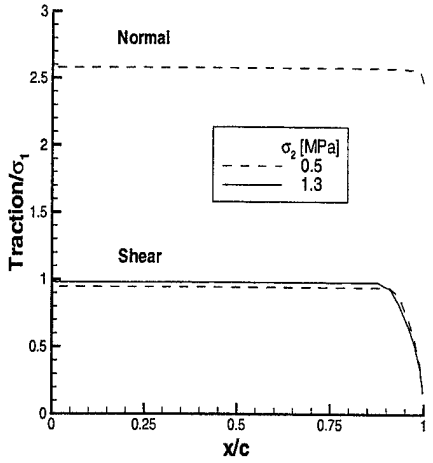

(a) Biaxial compression (b) Non-uniform surface roughness

Figure 7. Normal and frictional shear stresses along crack surfaces

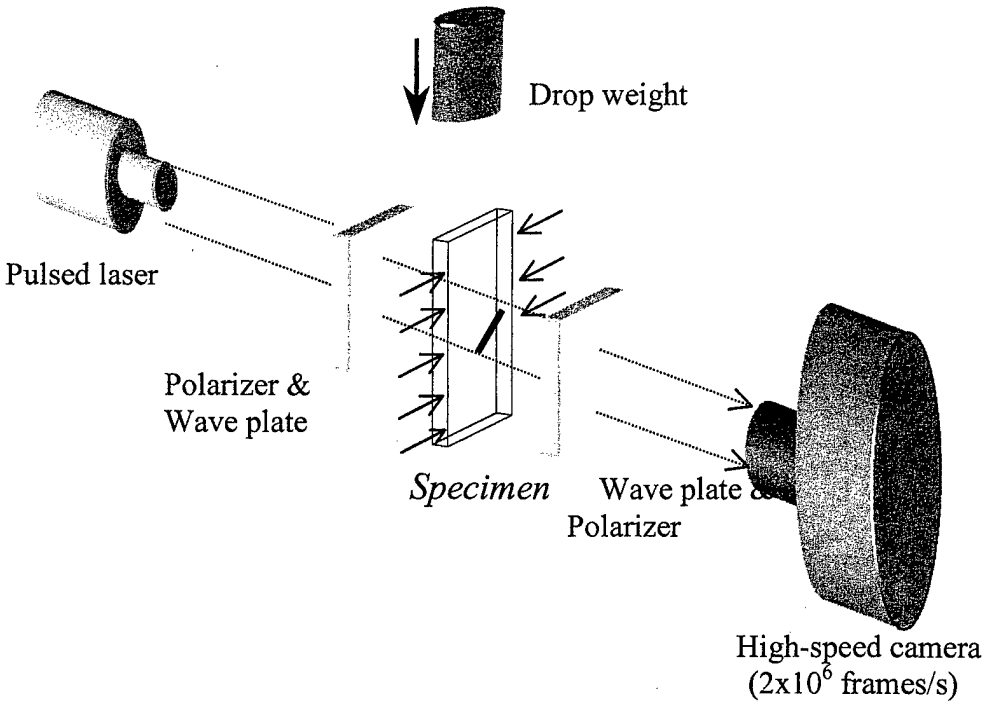

Figure 8. Experimental setup for impact tests.

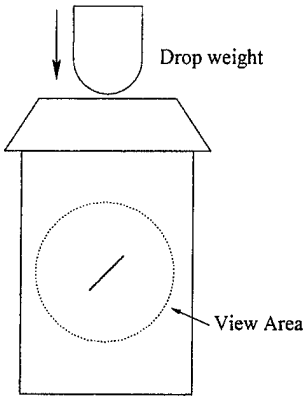

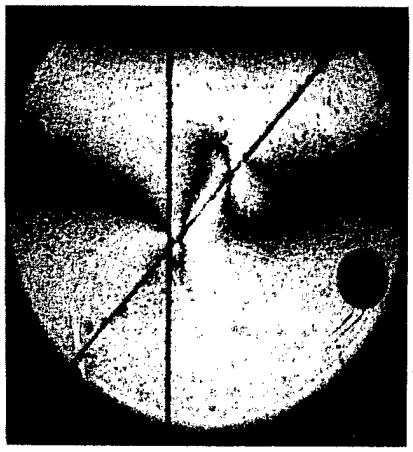

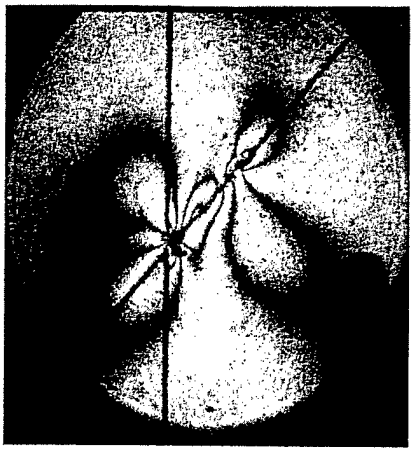

(a) t = 16.6μs after impact (b) Crack initiation (t = 49.8μs)

Figure 9. Isochrmatic fringes under uniaxial dynamic loading, μ = 0.3

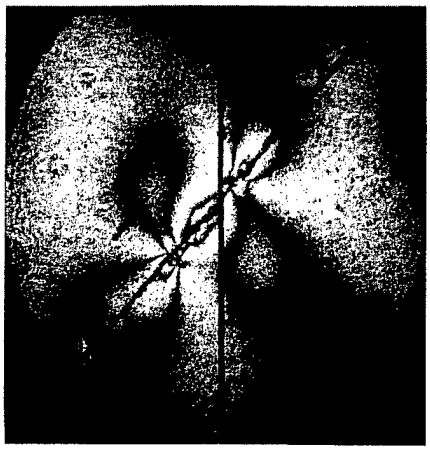

(a) t = 16.6μs after impact (b) Crack initiation (t = 49.8μs)

Figure 10. Isochrmatic fringes under uniaxial dynamic loading, μ = 0.70